MOL#25015

Human RNase H1 discriminates between subtle variations in the structure of the heteroduplex substrate

Walt F. Lima, John B. Rose, Josh G. Nichols, Hongjiang Wu, Michael T. Migawa,

Tadeusz K. Wyrzykiewicz, Andrew M. Siwkowski and Stanley T. Crooke

Department of Molecular and Structural Biology

Isis Pharmaceuticals

1

MOL#25015

Running title: Influence of substrate structure on human RNase H1 activity

Corresponding author:

Walt F. Lima

2292 Faraday Ave.

Carlsbad, CA. 92008

Ph. (760) 603-2387

Fax (760) 931-0209

Email: wlima@isisph.com

Text pages: 39

Figures: 5

References: 39

Abstract: 243 words

Introduction: 748 words

Discussion: 1424 words

Abbreviations: ASO, antisense oligonucleotide

Abstract

In a previous study we demonstrated that the sugar conformation and helical
geometry of the heteroduplex substrate at the catalytic site of human RNase H1
directs the selective recognition of the substrate by the enzyme (Lima WF,
Nichols JG, Wu H, Prakash TP, Migawa MT, Wyrzykiewicz TK, Bhat B and
Crooke ST (2004) *J. Biol. Chem.* 279: 36317-36326). Here, we systematically
introduced 2'-methoxyethoxy (MOE) nucleotides into the antisense
oligodeoxyribonucleotide (ASO) of the heteroduplex to alter the helical geometry
of the substrate. The MOE substitutions at the 3' and 5'-poles of the ASO
resulted in fewer cleavage sites and slower cleavage rates compared to the
unmodified substrates. Further, a greater reduction in cleavage activity was
observed for MOE substitutions at the 5'-pole of the ASO. The 3'-most and 5'-
most cleavage sites were positioned, respectively, 2 and 4-5 base-pairs from the
nearest MOE residues suggesting a conformational transmission of the
MOE/RNA helical geometry into the DNA/RNA portion of the heteroduplex.
Similar conformational transmission was observed for Okazaki-like substrates
containing deoxyribonucleotide substitutions at the 3'-pole of the
oligoribonucleotide. Finally, the heteroduplex substrates exhibited preferred
cleavage sites, which were cleaved 2 to 3-fold faster than other sites in the
substrate and these sites exhibited the greatest influence on the initial cleavage
rates. The data presented here offer further insights into the role substrate
structure plays in directing human RNase H1 activity as well as the design of
effective ASOs.

3

RNase H hydrolyzes RNA in RNA-DNA hybrids (Stein and Hausen, 1969).

RNase H enzymes function as endonucleases requiring divalent cations (e.g.,

Mg^{2+}, Mn^{2+}) to produce cleavage products with 5'-phosphate and 3'-hydroxyl

termini (Crouch and Dirksen, 1982). RNase H activity appears to be ubiquitous in

eukaryotes and bacteria (Itaya and Kondo, 1991; Itaya, 1991; Kanaya and Itaya,

1992; Busen, 1980; Rong and Carl, 1990; Eder, 1993). Two classes of RNase H

enzymes have been identified in mammalian cells (Busen, 1980; Eder, 1993; Wu,

1998; Masutani, 1990; Frank, 1994). Although the biological roles for the human

enzymes are not fully understood, RNase H2 appears to be involved in *de novo*

DNA replication and RNase H1 has been shown in mice to be important for

mitochondrial DNA replication (Busen, 1977; Turchi, 1994; Ceritelli, 2003). In

addition, human RNase H1 was shown to play a dominant role in the activities of

DNA-like antisense oligonucleotides (ASO) (Wu, 2004).

The structure of human RNase H1 consists of an RNA-binding domain

homologous with yeast RNase H1 that is separated from the catalytic domain by

a 62 amino acid spacer region (Wu, 2001; Cerritelli and Crouch, 1995; Evans

and Bycroft, 1999). The catalytic domain is highly conserved with the amino acid

sequences of other RNase H1 proteins and contains the key catalytic and

substrate binding residues required for activity (Wu, 2001; Kanaya, 1991;

Nakamura, 1991; Katayanagi, 1990; Yang, 1990). In addition, the catalytic

domain has been shown to contain a unique redox switch formed by adjacent

cysteine residues (Lima, 2003a). The spacer region has been shown to be

required for RNase H activity (Wu, 2001). Although the RNA-binding domain is

not required for RNase H activity, this region is responsible for the enhanced

binding affinity of the human enzyme for the heteroduplex substrate as well as

the strong positional preference for cleavage exhibited by the enzyme (Wu, 2001;

Lima, 2003b). Finally, the positional preference for cleavage is consistent with

the proposed biological role for mammalian RNase H1, i.e., the removal of RNA

primers during mitochondrial DNA synthesis (Ceritelli, 2003).

First generation phosphorotioate oligodeoxynucleotides have been shown to

induce pharmacological effects *in vivo* and to reduce target RNA in humans

(Yacyshyn, 1998). However they display significant limitations including limited

potency and the need to be given intravenously every other day. The 2'-

methoxyethoxy (MOE) modified chimeric ASOs are the product of more than a

decade of medicinal chemistry research of antisense oligonucleotides (for review

see Crooke, 2001). MOE modifications enhance affinity for target approximately

1 to 2° per modification, improve potency 10 to 40-fold and extend elimination

half-lives in all species including man from 14 to 30 days (For review see Crooke,

2001). MOE modified chimeric ASOs have also been shown to interact differently

with the Toll-like receptors than DNA ASOs and as a result are less pro-

inflammatory (For review see Crooke, 2001). Second generation MOE chimeric

ASOs currently in clinical trails are showing improved efficacy and therapeutic

indexes in man compared to first generation ASOs. For example, Isis 301012 an

inhibitor of apoB100 was shown to reduce apoB100 protein, low density

lipoprotein cholesterol (LDL), very low density lipoprotein (VLDL), total cholesterol and triglycerides in a dose dependant fashion with a minimum effective dose of 50 mg per week administered subcutaneously. Consistent with an elimination half-life of 31 days it produced effects that lasted as long as 3 months. More over it was extremely well tolerated (Kastelein, 2005). In addition, positive phase 2 results with patients with type 2 diabetes have been reported for the PTP-1B inhibitor Isis 113715 (Kjems, 2005). As another example, OGX-011 produced dose dependant reduction to greater than 90% of its target clusterin in prostate cancer and draining lymphnodes in patients with locally invasive prostate cancer (Chi, 2004).

The purpose of the present study was to extend our earlier observations and to provide a more precise understanding of the effects of MOE nucleotides on both the overall rate of cleavage and the precise positions of cleavage induced by human RNase H1. In a previous study we evaluated the effects of modified nucleotides positioned at sites on the substrate that interact directly with the enzyme (Lima, 2004). Here, we designed a series of chimeric ASOs to evaluate the local and long-range influence of the substrate structure on human RNase H1 activity. The 2'-methoxyethoxy (MOE) nucleotides were selected for this study as they have been shown to enhance the potency of ASOs through increased hybridization affinity and nuclease resistance (For review see Crooke, 2001).

Materials and Methods

Preparation of Human RNase H1.

Human RNase H1 containing an N-terminal His-tag was expressed and purified

as previously described (Lima, 2001). Briefly, the plasmids were transfected into

E. coli BL21 (DE3) (Novagen, WI). The bacteria was grown in Terrific Broth

medium (QBiogene, CA) at 37° C and harvested at OD_{600} of 1.2. The cells were

induced with 1 mM isopropylthiogalactoside (IPTG) at 37° C for 2 h. The cells

were lysed in 6 M guanidine hydrochoride 100 mM sodium phosphate, 10 mM

tris, pH 8.0 for 16 – 20 h at 24° C. The recombinant proteins were incubated for 1

h with 1 mL of Ni-NTA Super flow beads (Qiagen, CA) per 50 mL of lysate. The

Ni-NTA media was packed into an FPLC column and the RNase H1 proteins

partially purified with sequential gradients (flow rate, 5 mL/min; buffer A, 100 mM

sodium phosphate, 10 mM tris-HCl, 8 M Urea, pH 6.3; buffer B, 100 mM sodium

phosphate, 10 mM tris-HCl, 2 M Urea, pH 6.3; buffer C, 100 mM sodium

phosphate, 10 mM tris-HCl, 2 M Urea, 100 mM EDTA, pH 7.0). The eluent was

further purified by ion exchange FPLC chromatography using Mono S Column

(Amersham Pharmacia, Sweden); flow rate, 1 mL/min; buffer A, 20 mM sodium

phosphate, 2 M urea, 200 mM NaCl, pH 7.0; buffer B, 20 mM sodium phosphate,

2 M urea, 2 M NaCl, pH 7.0. Fractions containing RNase H1 were pooled and

concentrated. The concentrated protein was purified by RP-FPLC using

Resourse RPC Column (Amersham Pharmacia, Sweden); flow rate 1 mL/min;

Buffer A, 2% acetonirtile in diH_2O, 0.065% triflouroacetic acid; buffer B 80%

acetonitrile in diH$_2$O, 0.05% trifluoroacetic acid. Fractions were lyophilized,

resuspended in diH$_2$O and analyzed by SDS-PAGE.

Synthesis of oligonucleotides

Synthesis and purification of chimeric 2'-methoxyethoxy/deoxy

oligoribonuceotides were as previously described (Mckay, 199; Baker, 1997).

The oligoribonucleotides were synthesized on a PE-ABI 380B synthesizer using

5'-*O*-silyl-2'-*O*-bis(2-acetoxyethoxy)methyl ribonucleoside phosphoramidites and

procedures described elsewhere (Scaringe, 1998). The oligoribonucleotides were

purified by reverse-phase HPLC. The oligodeoxyribonucleotides were

synthesized on a PE-ABI 380B automated DNA synthesizer and standard

phosphoramidite chemistry. The oligodeoxyribonucleotides were purified by

precipitation 2 times out of 0.5 M NaCl with 2.5 volumes of ethyl alcohol. The

purified products were greater than 90% full length material as determined by

polyacrylamide gel electrophoresis analysis.

Preparation of ^{32}P labeled substrate

The RNA substrate was 5'-end-labeled with ^{32}P using 20 U of T4 polynucleotide

kinase (Promega, WI), 120 pmol (7000 Ci/mmol) [γ-^{32}P]ATP (ICN, CA), 40 pmol

RNA, 70 mM tris, pH 7.6, 10 mM MgCl$_2$ and 50 mM DTT. The kinase reaction

was incubated at 37° C for 30 min. The labeled oligoribonucleotide was purified

by electrophoresis on a 12% denaturing polyacrylamide gel (Sambrook, 1989).

The specific activity of the labeled oligonucleotide is approximately 3000 to 8000 cpm/fmol.

Preparation of the heteroduplexes

The heteroduplex substrate was prepared in 100 µL containing 500 nM unlabeled oligoribonucleotide, 10^5 cpm of ^{32}P labeled oligoribonucleotide, two-fold excess complementary oligodeoxyribonucleotide and hybridization buffer [20 mM tris, pH 7.5, 20 mM KCl]. Reactions were heated at 90° C for 5 min, cooled to 37° C. Hybridization reactions were incubated 2 - 16 h at 37° C and 1 mM tris(2-carboxyethyl)phosphate (TCEP), 1 mM MgCl$_2$ and 60 U of Prime RNase Inhibitor (5 Prime $\rightarrow$ 3 Prime, CO) was added.

Multiple-turnover kinetics

The human RNase H1 proteins were incubated with dilution buffer (50 mM tris, 50 mM NaCl, 100 µM TCEP, pH 7.5) for 1 h at 37° C. The heteroduplex substrate was digested with 0.4 ng of enzyme at 37° C. A 10 µl aliquot of the cleavage reaction was removed at time points ranging from 2 - 120 min and quenched by adding 10 µL of stop solution (8 M urea and 120 mM EDTA). The aliquots were heated at 90° C for 2 min, resolved in a 12% denaturing polyacrylamide gel and the substrate and product bands were quantitated on a Molecular Dynamics PhosphorImager. The concentration of the converted product was plotted as a function of time. The initial cleavage rate (V_0) was obtained from the slope (nmol RNA cleaved/min) of the best-fit line for the linear portion of the plot, which

9

comprises, in general < 10% of the total reaction and data from at least five time points.

Cell culture and treatment

ASOs were transfected into mouse brain endothelial (bEND) cells, obtained from the American Type Culture Collection, using 3ug/ml Lipofectin (Invitrogen) in OptiMem (Invitrogen) for 4 hrs. Transfection mixes were then exchanged with normal growth medium (DMEM-high glucose containing 10% FBS, all from Invitrogen) and cells incubated for 48 hrs prior to RNA harvest. RNA was purified using an RNeasy 96-well plate(Qiagen) according to manufacturer's protocol and eluted in water. RNA was analyzed by quantitative RT-PCR using an ABI-Prism 7700. TRADD RNA levels were normalized to those of cyclophilin A, a housekeeping gene. Primers used for determination of TRADD RNA level are as follows: forward primer (FP) 5' GGCCGCCTGCCAGAC 3', reverse primer (RP) 5' TGAAGAGTCAGTGGCCGGTT 3', and probe (PR) 5' 6FAM-TTTCTGTTCCACGGGCAGCTCGTAGT-TAMRA 3'. Primers used for determination of cyclophilin A RNA level are as follows: FP 5' TCGCCGCTTGCTGCA 3', RP 5' ATCGGCCGTGATGTCGA 3', and PR 5' 6FAM-CCATGGTCAACCCCACCGTGTTC-TAMRA 3'. Values shown represent the average ± standard deviation (n=3 per treatment group).

Results

Effects of successive MOE substitutions positioned at the 3' and 5'-poles of the ASO

The cleavage sites of the heteroduplex A substrates in which the deoxyribonucleotides were successively substituted with MOE modified residues at the 3'-pole of the ASO are shown in Figure 1A. Human RNase H1 cleavage of the unmodified heteroduplex A resulted in a broad cleavage pattern consisting of 10 cleavage sites with the 5'-most and 3'-most cleavage sites, respectively, 6 and 15 residues from the 5'-terminus of the oligoribonucleotide (Fig. 1A). The unmodified heteroduplex A also exhibited several preferred human RNase H1 cleavage sites, i.e., sites cleaved 2 to 3-fold faster than other sites by the enzyme. For example, preferred cleavage sites were observed at ribonucleotides 7, 8, 9, 11 and 15 from the 5'-terminus of the RNA. Heteroduplexes in which the first one or two 3'-nucleotides were MOE residues (19-1 and 18-2) exhibited a similar number of cleavage sites compared to the unmodified heteroduplex (Fig. 1A). Ablation of the 5'-most cleavage site in the oligoribonucleotide was observed for the heteroduplex containing three MOE residues at the 3'-terminus of the ASO (Fig. 1A). Each additional MOE substitution resulted in a concomitant ablation of the 5'-most cleavage site in the oligoribonucleotide resulting in a 4 – 5 base-pair separation between the 5'-most cleavage site and the 5'-terminal MOE residue with greater than eleven MOE substitutions resulting in the loss of all the human RNase H1 cleavage sites.

The cleavage rate for the 19-1 heteroduplex containing a single MOE positioned at the 3'-terminus of the ASO was 31% slower than the unmodified heteroduplex A (Fig. 1A). Two MOE substitutions at the 3'-terminus of the ASO (18-2) resulted in a cleavage rate approximately 50% slower than the cleavage rate for the unmodified heteroduplex. No further reduction in the cleavage rate was observed for the heteroduplexes containing three to eleven MOE residues at the 3'-pole of the ASO irrespective of the number of cleavage sites. In addition, the MOE residues at the 3'-pole of the ASO produced new preferred cleavage sites 3' on the RNA (Fig. 1A). For example, one human RNase H1 cleavage site on the 11-9 heteroduplex accounted for an initial cleavage rate comparable to the 16-4 heteroduplex with eight cleavage sites.

The effect of MOE substitutions at the 5'-pole of the ASO on the cleavage patterns and initial cleavage rates are shown in figure 1B. Similar numbers of cleavage sites were observed for the unmodified substrate and heteroduplexes containing one to three MOE residues at the 5'-terminus of the ASO (Fig. 1B). Four MOE residues at the 5'-pole of the ASO resulted in the ablation of the 3'-cleavage site on the RNA. Additional MOE substitutions at the 5'-pole of the ASO resulted in a concomitant ablation of the 3'-most cleavage site in the RNA (Fig. 1B). The cleavage pattern for the heteroduplexes containing greater than three MOE residues at the 5'-pole of the oligodeoxyribonucleotide showed a consistent two base-pair separation between the 3'-cleavage site on the RNA and the 3'-terminal MOE nucleotide on the ASO (Fig. 1B). In contrast to the observations

12

with MOE modifications positioned at the 3'-pole of the oligodeoxyribonucleotide,
fewer cleavage sites resulted in slower overall cleavage rates. For example, a
70% reduction in the cleavage rate was observed for the 10-10 heteroduplex
containing three cleavage sites compared to the unmodified substrate with ten
cleavage sites. In this case, the successive ablation of the 5'-most cleavage sites
did not produce an enhanced rate for the remaining cleavage sites. Finally,
similar reductions in the cleavage rates were observed for the heteroduplexes
containing two MOE substitutions at either the 3' or 5'-termini of the ASO (Fig. 1A
and B).

Effects of heteroduplex length

Given that the MOE substitutions at the 3'- and 5'-poles of the ASO effectively
shortened the length of the RNA/DNA region of the chimeric substrates, we
evaluated the influence of RNA/DNA length on human RNase H1 activity (Fig. 2).
Specifically, the sequence of the heteroduplex A was either shortened (A-10 and
A-15) or extended (A-30 and A-40) from the 3'-RNA/5'-DNA terminus of the
parent 20 Base-pair sequence (A-20) (Fig. 2). The 5'-most cleavage site was
consistently positioned 6 ribonucleotides from the 5'-terminus of the RNA. In
contrast, the position of the 3'-most cleavage site on the RNA was dependent on
the length of the heteroduplex. For example, the 3'-cleavage sites for the 10 and
15 base-pair heteroduplexes were positioned 4 ribonucleotides from the 3'-
terminus of the RNA whereas, the distance between the 3'-most cleavage site

and the 3'- terminus of the RNA increased to 6, 7 and 10 ribonucleotides,

respectively, for the 20, 30 and 40 base-pair substrates (Fig. 2). The positions of

the preferred cleavage sites were also dependent on the length of the

heteroduplex. The greatest human RNase H1 activity was observed at

ribonucleotides 6 and 7 from the 5'-terminus of the RNA for the 10 base-pair

heteroduplex and ribonucleotides 6, 7, 8 and 11 for the15 base-pair substrate.

Additional preferred cleavage sites were observed 3' on the RNA for the 20, 30

and 40 base-pair substrates. For example, preferred cleavage sites were

observed at ribonucleotides 21 and 23 for the 30 base-pair heteroduplex and 30,

33 and 34 for the 40 base-pair heteroduplex.

Effects of heteroduplex sequence

The cleavage patterns and cleavage rates for various RNA/DNA heteroduplex

sequences are shown in figure 3A. Heteroduplex A exhibited an unusually broad

cleavage pattern with numerous preferred cleavage sites (Fig. 1). This unique

cleavage pattern resulted in greatest initial cleavage rate among the

heteroduplexes tested. In contrast, the other heteroduplexes displayed a

narrower cleavage pattern with fewer preferred cleavage sites positioned

predominantly within the preferred position for cleavage, i.e., 7 to 12

ribonucleotides from the 5'-terminus of the RNA. An approximate 2-fold slower

cleavage rates were observed for these heteroduplexes compared to the

heteroduplex A substrate.

Effects of 2'-MOE substitutions positioned at both the 3' and 5'-poles of the ASO

Cleavage sites and rates for the chimeric heteroduplexes in which the RNA/DNA region was positioned either centrally (5-10-5) or toward the 3'-pole of the RNA (2-10-8) are shown in Figure 3A. The cleavage sites for the 5-10-5 heteroduplexes were shifted 3' on the RNA compared with the unmodified substrates. A further shift 3' in the RNA was observed for the cleavage sites of the 2-10-8 heteroduplexes (Fig. 3A). Consistent with the successive MOE substitutions in the ASO (Fig. 1A), the 5-10-5 and 2-10-8 heteroduplexes exhibited a 4 to 5 base-pair separation from the 5'-most cleavage site on the RNA and the nearest MOE at the 3'-pole of the ASO (Fig. 3A). Similarly, a two base-pair separation was observed between the 3'-most cleavage site on the RNA and the nearest MOE at the 5'-pole of the ASO. The greatest loss in human RNase H1 activity compared to the unmodified substrate was observed for the 5-10-5 chimeric heteroduplex A. The reduction in activity appeared to be due to the failure to generate a preferred cleavage site within the RNA/DNA portion of the chimeric substrate. Similarly, no preferred cleavage sites were observed for either the 5-10-5 or 2-10-8 heteroduplexes D resulting in a greater than two fold reduction in the initial cleavage rate compared to the unmodified heteroduplex D even though both chimeric heteroduplexes exhibited a greater number of cleavage sites compared to the unmodified heteroduplex D (Fig. 3A). In the case of heteroduplex C, new preferred cleavage sites were observed for the 5-10-5

heteroduplex resulting in a cleavage rate comparable to the unmodified

heteroduplex, whereas the 2-10-8 heteroduplex showed fewer cleavage sites

resulting in a 3-fold slower cleavage rate compared to either the 5-10-5 or

unmodified heteroduplexes. In contrast, the 5-10-5 chimeric heteroduplex B

exhibited a similar number of preferred cleavage sites compared to the

unmodified heteroduplex B resulting in an initial cleavage rate comparable to the

unmodified substrate. Again, the number of preferred cleavage sites appears to

have a greater effect on the initial cleavage rates for the various chimeric

heteroduplexes than the total number of cleavage sites.

The sequences were chosen based on active ASO binding sites identified from

ASO transfection of cultured cells (data not shown). To compare the effects of

MOE substitutions in the ASO on human RNase H1 activity with the gene

silencing activities of the ASOs in cells, we transfected the 5-10-5 and 2-10-8

ASOs of heteroduplex C into bEND cells and measured the intracellular

concentrations of the target mRNA, in this case TRADD mRNA. The

heteroduplex C ASOs were chosen because these heteroduplexes showed the

greatest difference in human RNase H1 activity for ASOs containing the same

number of MOE residues and therefore likely exhibit similar binding affinities for

the mRNA target (Fig. 3A). Consistent with the reduction in cleavage rate

observed for the 2-10-8 Heteroduplex C compared to either the 5-10-5 or

unmodified heteroduplexes, the 2-10-8 ASO was also less potent than the 5-10-5

ASO at reducing TRADD mRNA levels in the cell (Fig. 4). Interestingly, a greater

reduction in activity was observed in cells, (e.g., a 6-fold difference in IC_{50} was observed for the 2-10-8 and 5-10-5 ASOs compared to the 3-fold difference in the human RNase H1 cleavage rate) (fig. 3A and 4).

To evaluate both the influence of the MOE modifications and the contribution of heteroduplex sequence on human RNase H1 cleavage rates, unmodified heteroduplexes were prepared with the 5'-termini of the ASO positioned to match the 3'-MOE/5'-DNA junction of the 5-10-5 chimeric heteroduplexes (Fig. 2B). The length of the ASO was either ten nucleotides to match the DNA portion of the 5-10-5 chimeric oligodeoxyribonucleotide or 20 nucleotides to match the unmodified substrate. In all cases, the initial cleavage rates for the unmodified heteroduplexes were significantly greater than the cleavage rates observed for the 5-10-5 heteroduplexes (Fig. 3B). Although similar cleavage patterns were observed for the 5-10-5 heteroduplexes and the unmodified heteroduplexes containing ten deoxyribonucleotides, the RNase H1 activity at the cleavage sites of the unmodified heteroduplexes containing ten deoxyribonucleotides were significantly greater compared with the 5-10-5 heteroduplexes. For example, two cleavage sites were observed for the 5-10-5 and unmodified heteroduplexes B and E containing ten deoxyribonucleotides. Yet, the unmodified substrates exhibited significantly greater human RNase H1 activity at those sites, resulting in a 3-fold increase in the initial cleavage rates compared to the 5-10-5 chimeric heteroduplexes. In contrast, the heteroduplexes containing 20 deoxyribonucleotides exhibited additional cleavage sites 3' on the RNA

compared to the 5-10-5 and ten deoxyribonucleotide heteroduplexes, although

comparable cleavage rates were observed for the unmodified heteroduplexes

containing 10 and 20 deoxyribonucleotides (Fig. 3B). These data suggest that

the slower cleavage rates observed for the 5-10-5 heteroduplexes compared to

the unmodified substrates were due to the MOE substitutions and not to the

length of the deoxyribonucleotide region of the ASO.

Okazaki-like substrates were prepared with a oligodeoxyribonucleotide annealed

to a complementary RNA/DNA chimeric oligonucleotide containing 10 (A-10/10)

and 15 (A-15/5) ribonucleotides at the 5'-pole and, respectively, 10 and 5

contiguous deoxyribonucleotides extending 3' (Fig. 5). Deoxyribonucleotide

substitutions at the 3'-pole of the oligoribonucleotide resulted in a loss of the 3'-

most cleavage site and an increase in the cleavage rates for the remaining sites

(Fig. 5). In other words, the successive ablation of the 3'-most cleavage sites

produced new preferred cleavage sites resulting in comparable cleavage rates

for the A-10/10, A-15/5 and unmodified heteroduplexes.

Discussion

Heteroduplex sequence and structure affect cleavage sites and rates

Certain human RNase H1 cleavage sites appeared to be preferentially cleaved

exhibiting 2 to 3-fold greater activity compared to the other cleavage sites (Fig. 1,

18

2 and 3). In addition, these preferred cleavage sites provided the greatest contribution to the overall cleavage rate. No consensus sequence was observed for the preferred human RNase H1 cleavage sites (Fig. 1, 2 and 3). Instead, the position of the preferred cleavage sites in the heteroduplex substrate is consistent with the strong positional preference for cleavage observed for the enzyme, i.e., human RNase H1 preferentially cleaves the heteroduplex substrate 7 to 10 nucleotides from the 5'-RNA/3'-DNA terminus, (Wu, 1999; Lima, 2003a). With the exception of heteroduplex A, the preferred cleavage sites observed for the various heteroduplex sequences were positioned within this 7 to 10 nucleotide region (Fig. 3A).

The lack of a consensus sequence for the preferred cleavage sites is likely due to the binding interaction between the enzyme and substrate which is predicted to comprise approximately one helical turn of the heteroduplex substrate (Lima, 2003b; Lima, 2004). Consequently, the preferred cleavage sites are the product of the sequence/helical geometry of the heteroduplex region interacting with the enzyme. Consistent with these observations, proteins involved in the small interfering RNA (siRNA) pathway have been shown to measure subtle sequence dependant differences in the helical geometry of oligoribonucleotide duplexes (Tomari, 2004). For example, the Dicer-2/R2D2 heterodimer was shown to orient the siRNA for loading into the RNA-induced silencing complex (RISC) based on subtle thermodynamic differences of the terminal base-pairs. The complexity of these interactions is further emphasized by the results shown in figure 2. In

19

theory, as the length of the heteroduplex was increased, cleavage sites should

have expanded relatively uniformly since all of the experiments were in substrate

excess. In contrast, as the heteroduplexes were lengthened, we observed areas

in which there was essentially no cleavage as well as new sites of preferred

cleavages.

MOE substitutions inhibit human RNase H1 activity

The human RNase H1 cleavage rates for the chimeric substrates containing

deoxyribonucleotides flanked on both ends with MOE residues were slower than

the cleavage rates observed for substrates containing similar RNA/DNA regions

without MOE residues (Fig. 3). Several factors appear to contribute to the

reduction in human RNase H1 activity. First, several chimeric heteroduplexes

redirected the position of cleavage outside the positional preference for cleavage,

(e.g., the 2-10-8 chimeric heteroduplexes B, C, D and E) resulting in fewer

preferred cleavage sites and slower overall cleavage rates (Fig. 3A). Importantly,

the reduction in human RNase H1 activity observed for the 2-10-8 of

heteroduplex C was consistent with a reduction potency observed for this ASO in

cultured cells compared to the 5-10-5 ASO (Fig. 4).

Second, the reduction in human RNase H1 activity observed for the chimeric

heteroduplexes appeared to be primarily due to the MOE substitutions and not

the shorter length of the deoxyribonucleotide region of the chimeric

heteroduplexes as comparable cleavage rates were observed for the

heteroduplexes containing the 10 and 20 deoxyribonucleotides without flanking

MOE residues (Fig. 3B). The influence of the MOE substitutions on human

RNase H1 activity is consistent with the solution structure of a chimeric

heteroduplex containing deoxyribonucleotides flanked on both ends with 2'-

methoxy residues hybridized to RNA (Nishizaki, 1997). Specifically, the central

deoxyribonucleotides exhibited the eastern biased sugar conformation preferred

by RNase H1 whereas the flanking 2'-methoxy residues exhibited a northern

sugar conformation. Importantly, the deoxyribonucleotides adjacent the 2'-

methoxy residues also were shown to exhibit a northern sugar conformation

suggesting the conformational transmission of the northern biased 2'-methoxy

residues into adjacent deoxyribonucleotides (Nishizaki, 1997). Given that

heteroduplexes containing northern biased nucleotides within the DNA strand do

not support human RNase H1 activity (Lima, 2004), the attenuation of the human

RNase H1 activity observed for the chimeric heteroduplexes is likely due to the

conformational transmission of the northern biased MOE residues into the

adjacent deoxyribonucleotides.

Third, the influence of the MOE residues on human RNase H1 activity was

directional (Fig. 1). The observed differences in activity between chimeric

heteroduplexes containing MOE residues at the 5'-pole of the DNA strand

compared to the 3'-pole is likely due to the binding directionality of the enzyme.

Human RNase H1 is predicted to position the catalytic domain 3' on the RNA

relative to the RNA binding-domain (Fig. 6). As a result, MOE substitutions at the 3'-pole of the oligodeoxyribonucleotide would be positioned at the RNA binding-domain and the MOE modifications at the 5'-pole would be positioned adjacent to the catalytic domain of the enzyme (Fig. 6). Given that the RNA binding domain of human RNase H1 has been shown to be important for properly positioning the enzyme on the heteroduplex for catalysis (Lima, 2003a), MOE substitutions at the 3'-pole of the oligodeoxyribonucleotide likely interfere with the binding of the enzyme to this portion of the substrate, effectively redirecting the enzyme to the RNA/DNA region of the chimeric heteroduplex (Fig. 1A and 6). Consistent with this model, MOE substitutions at the 5'-pole of the oligodeoxyribonucleotide would interfere with the catalytic domain of the enzyme, resulting in the observed progressive ablation of human RNase H1 cleavage sites without the concomitant production of new preferred cleavage sites (Fig. 1B and 6).

Human RNase H1 is optimally evolved to cleave Okazaki fragments

A recent study demonstrated that RNase H1 is required for mitochondrial DNA replication and plays a critical role in the embryonic development of mice (Ceritelli, 2003). The enzyme is believed to participate in the removal of RNA primers during lagging strand DNA synthesis (Busen, 1977; Turchi, 1994; Ceritelli, 2003). Therefore, the proposed native substrates for the enzyme are chimeric heteroduplexes consisting of 7 to 14 ribonucleotide primers with contiguous stretches of DNA extending 3', hybridized to DNA (Bambara, 1997).

Consistent with the proposed biological role for the enzyme, the Okazaki-like substrates containing 5 and 10 deoxyribonucleotides at the 3'-pole of the oligoribonucleotide produced new preferred cleavage sites and exhibited cleavage rates comparable to the unmodified heteroduplex (Fig. 5). Considering that the short RNA primers are interspersed within long stretches of dsDNA, the model proposed here for the interaction between the enzyme and the heteroduplex substrate correlates well with biological role for the enzyme (Fig. 6). First, the strong positional preference for cleavage is consistent with the length of the RNA primers. Second, human RNase H1 binds the RNA/DNA heteroduplex approximately 50-fold tighter than dsDNA suggesting that the enzyme would not be trapped in nonproductive interactions within the large field of dsDNA (Wu, 1999). Third, the limited sequence discrimination exhibited by the enzyme would be beneficial given that the RNA primers comprise mixed sequences. Finally, DNA substitutions appeared to affect human RNase H1 activity differently than MOE substitutions. Although both the DNA and MOE substitutions resulted in a similar shift in the position of cleavage and few cleavage sites compared to the unmodified substrate, the MOE substitutions resulted in slower overall cleavage rates whereas the DNA substitutions generated new preferred cleavage sites. The differences in activity are likely due to the differences in the sugar conformation as well conformational transmission of the MOE and DNA residues.

The design of improved DNA-like ASOs

The observations presented here combined with the demonstration that human RNase H1 plays a dominant role in the activities of DNA-like ASOs offer approaches to enhance the design of effective chimeric ASOs (Lima, 2003b). Although the endogenous ASO/mRNA structures contain ssRNA regions extending from both termini of the ASO, the cleavage patterns observed for the chimeric ASOs with flanking 2'-modifications suggest that the ssRNA regions would have no effect on the activity of the enzyme (Fig. 3). In fact, identical cleavage sites to those observed for the 5-10-5 heteroduplex E were also observed for the endogenous target mRNA from human cells transfected with the 5-10-5 chimeric ASO of heteroduplex E using RNA ligase mediated rapid amplification of 5'-cDNA ends (5'-RACE) (Barnes, 1994) (data not shown). Most importantly, the observed influence of the MOE substitutions of on human RNase H1 activity suggests that reducing the number 2'- modified nucleotides should improve the enzyme activity. Obviously, as 2'- modified nucleotides improve affinity to target RNA, reducing the number of 2'- modified nucleotides would reduce the ability of the ASO to invade structured RNA sites resulting in fewer active sites in the mRNA. However, once hybridization is accomplished, RNase H1 activity becomes limiting so fewer 2'-MOE residues should result in greater ASO potency (Lima, 2003b). Finally, inserting modified nucleotides to modulate the transmission of the 2'-modified/RNA geometry into the RNA/DNA portion of the chimeric heteroduplex should also improve human RNase H1 activity.

References

Baker BF, Lot SS, Condon TP, Cheng-Flournoy S, Lesnik EA, Sasmor HM and

Bennett, CF (1997) 2'-O-(2-Methoxy)ethyl-modified anti-intercellular adhesion

molecule 1 (ICAM-1) oligonucleotides selectively increase the ICAM-1 mRNA

level and inhibit formation of the ICAM-1 translation initiation complex in human

umbilical vein endothelial cells. *J. Biol. Chem.* **272**: 11994-12000

Bambara RA, Murante RS and Hendriksen LA (1997) Enzymes and reactions at

the eukaryotic DNA replication fork. *J. Biol. Chem.* **272**: 4647-4650

Barnes WM (1994) PCR amplification of up to 35-kb DNA with high fidelity and

high yield from lambda bacteriophage templates. *Proc. Natl. Acad. Sci. U.S.A.* **91**:

2216-2219

Bradley JD, Graham M, Henry S, Kim TW, Crooke R, Yu R and de Haan H (2004)

Evaluation of ISIS 301012, an Antisense Inhibitor to Human apoB-100 in Healthy

Volunteers. Oral presentation at XV International Symposium on Drugs Affecting

Lipid Metabolism, Venice (Italy)

Busen W, Peter JH and Hausen P (1977) Ribonuclease H levels during the

response of bovine lymphocytes to concanavalin A. *Eur. J. Biochem.* **74**: 203-208

Busen W (1980) Purification, subunit structure, and serologicai analysis of calf

thymus ribonuclease H I. *J. Biol. Chem.* **255**: 9434-9443

Cerritelli SM and Crouch RJ (1995) The non-RNase H domain of Saccharomyces

cerevisiae RNase H1 binds double-stranded RNA: magnesium modulates the

switch between double-stranded RNA binding and RNase H activity. *RNA* **1**: 246-

259

Ceritelli SM, Frolova EG, Feng C, Grinberg A, Love PE and Crouch RJ (2003)

Failure to produce mitochondrial DNA results in embryonic lethality in Rnaseh1

null mice. *Molecular Cell* **11**: 807-815

Chi KN, Eisenhauer E, Fazli L, Jones EC, Powers J, Ayers D, Goldenberg SL

and Gleave ME (2004) A phase 1 pharmacokinetic and pharmacodynamic study

of OGX-011, a 2'-methoxyethyl phosphorothioate antisense oligonucleotide to

Clusterin, in patients with prostrate cancer prior to radical prostatectomy.

Presented at the American Society of Clinical Oncology.

Crooke ST (2001) in *Antisense Technology Principles, Strategies and*

Applications (Crooke ST ed) pp 1-28, Marcel Dekker Inc, New York.

Crooke RM (2005) Antisense oligonucleotides as therapeutics for

hyperlipidaemias. *Expert. Opin. Biol. Ther.* **7**: 907-17.

27

Crouch RJ and Dirksen ML (1982) *in* Nucleases (Linn SM and Roberts RJ Eds.)

pp 211-241, Cold Spring Harbor Laboratory press, Plainview, NY.

Eder PS, Walder RT and Walder JA (1993) Substrate specificity of human

RNase H1 and its role in excision repair of ribose residues misincorporated in

DNA. *Biochimie* **75**: 123-126

Evans SP and Bycroft M (1999) NMR structure of the N-terminal domain of

Saccharomyces cerevisiae RNase HI reveals a fold with a strong resemblance to

the N-terminal domain of ribosomal protein L9. *J. Mol. Biol.* **291**: 661-669

Frank P, Albert S, Cazenave C and Toulme JJ (1994) Purification and

characterization of human ribonuclease HII. *Nucleic Acids Res.* **22**: 5247-5254

Itaya M and Kondo K (1991) Molecular cloning of a ribonuclease H (RNase HI)

gene from an extreme thermophile Thermus thermophilus HB8: a thermostable

RNase H can functionally replace the Escherichia coli enzyme in vivo. *Nucleic Acids Res.* **19**: 4443-4449

Itaya M, McKelvin D, Chatterjie SK and Crouch RJ (1991) Selective cloning of genes encoding RNase H from Salmonella typhimurium, Saccharomyces cerevisiae and Escherichia coli rnh mutant. *Mol. Gen. Genet.* **227**: 438-445

Kanaya S, Katsuda-Kakai C and Ikehara M (1991) Importance of the positive charge cluster in Escherichia coli ribonuclease HI for the effective binding of the substrate. *J. Biol. Chem.* **266**: 11621-11627

Kanaya S and Itaya M (1992) Expression, purification, and characterization of a recombinant ribonuclease H from Thermus thermophilus HB8. *J. Biol. Chem.* **267**: 10184-10192

MOL#25015

Kastelein JP, Wedel MK, Baker BF, Su J, Bradley JD, Yu RZ, Chuang E,

Graham MJ and Crooke RM (2005) Potent Reduction of Apolipoprotein B and

LDL Cholesterol by Short-term Administration of an Antisense Inhibitor of

Apolipoprotein B. *Circulation,* in press*.*

Katayanagi K, Miyagawa M, Matsushima M, Ishkiawa M, Kanaya S, Ikehara M,

Matsuzaki T and Morikawa K (1990) Three-dimensional structure of ribonuclease

H from E. coli. *Nature* **347**: 306-309

Kjems LL, Bhanot S, Bradley JD, Monia B, Kwoh J and Wedel M (2004)

Increased Insulin Sensitivity in Humans by Protein Tyrosine Phosphatase 1B

(PTP-1B); Inhibition-Evaluation of ISIS 113715, an Antisense Inhibitor of PTP-1B.

Diabetes 54 (suppl. 1):A530

Lima WF, Wu H and Crooke ST (2001) *in "Methods in Enzymology"* (Nicholson

AW Ed.) pp 430-9, Academic Press, San Diego, CA

Lima WF, Wu H, Nichols JG, Manalili SM, Drader JJ, Hofstadler SA and Crooke

ST (2003a) Human RNase H1 activity is regulated by a unique redox switch

formed between adjacent cysteines. *J. Biol. Chem.* **278**: 14906-14912

Lima WF, Wu H, Nichols J, Prakash TP, Ravikumar V and Crooke ST (2003b)

Human RNase H1 uses one tryptophan and two lysines to position the enzyme at

the 3'-DNA/5'-RNA terminus of the heteroduplex substrate. *J. Biol. Chem.* **278**:

49860-49867

Lima WF, Nichols JG, Wu H, Prakash TP, Migawa MT, Wyrzykiewicz TK, Bhat B

and Crooke ST (2004) Structural requirements at the catalytic site of the

heteroduplex substrate for human RNase H1 catalysis. *J. Biol. Chem.* **279**:

36317-36326

MOL#25015

Masutani C, Enomoto T, Suzuki M, Hanaoka F and Ui M (1990) DNA primase

stimulatory factor from mouse FM3A cells has an RNase H activity. Purification of

the factor and analysis of the stimulation. *J. Biol. Chem.* **265**: 10210-10216

Mckay R, Miraglia L, Cummins L, Owens S, Sasmor H M and Dean N M (1999)

Characterization of a potent and specific class of antisense oligonucleotide

inhibitor of human protein kinase C-alpha expression. *J. Biol. Chem.* **274**: 1715-

1722

Nakamura H, ODA Y, Iwai S, Inoue H, Ohtsuka E, Kanaya S, Kimura S, Katsuda

C, Katayanagi K, Morikawa K, Miyashiro H and Ikehara M (1991) How does

RNase H recognize a DNA.RNA hybrid? *Proc. Natl. Acad. Sci. U. S. A.* **88**:

11535-11539

MOL#25015

Nishizaki T, Iwai S, Ohtsuka E and Nakamura H (1997) Solution structure of an RNA.2'-O-methylated RNA hybrid duplex containing an RNA.DNA hybrid segment at the center. *Biochemistry* **36**: 2577-2585

Ohtani N, Haruki M, Morikawa M, Crouch RJ, Itaya M and Kanaya S (1999) Identification of the genes encoding Mn2+-dependent RNase HII and Mg2+-dependent RNase HIII from Bacillus subtilis: classification of RNases H into three families. *Biochemistry* **38**; 605-618

Rong YW and Carl PL (1990) On the molecular weight and subunit composition of calf thymus ribonuclease H1. *Biochemistry* **29**; 383-389

Sambrook J, Fritsch EF and Maniatis T (1989) in *Molecular Cloning. A Laboratory Manual,* 2nd sd., Cold Spring Harbor Laboratory Press, Cold Spring Harbor, NY

Scaringe SA (2001) RNA oligonucleotide synthesis via 5'-silyl-2'-orthoester

chemistry. *Methods* **23**: 206-7

Stein H and Hausen P (1969) Enzyme from calf thymus degrading the RNA

moiety of DNA-RNA Hybrids: effect on DNA-dependent RNA polymerase.

Science **166**: 393-395

Tomari Y, Matranga C, Haley B, Martinez N and Zamore PD (2004) A protein

sensor for siRNA asymmetry. *Science* **306**: 1377-1380

Turchi JJ, Huang L, Murante, RS, Kim Y and Bambara RA (1994) Enzymatic

completion of mammalian lagging-strand DNA replication. *Proc. Natl. Acad. Sci.*

U.S.A. **91**: 9803-9807

Wu H, Lima WF and Crooke, ST (1998) Molecular Cloning and Expression of

cDNA for Human RNase H. *Antisense Nucleic Acid Drug Dev.* **8**: 53-61

Wu H, Lima WL and Crooke ST (1999) Properties of cloned and expressed human RNase H1. *J. Biol. Chem.* **274**: 28270-2827

Wu H, Lima WF and Crooke, ST (2001) Investigating the structure of human RNase H1 by site-directed mutagenesis. *J. Biol. Chem.* **276**: 23547-23553

Wu H, Lima WF, Zhang H, Fan A, Sun H and Crooke ST (2004) Determination of the role of the human RNase H1 in the pharmacology of DNA-like antisense drugs. *J. Biol. Chem.* **279**: 17181-17189

Yacyshyn BR, Bowen-Yacyshyn MB, Jewell L, Tami JA, Bennett CF, Kisner DL, Shanahan WR (1998) A placebo-controlled trial of ICAM-1 antisense oligonucleotide in the treatment of Crohn's disease. *Gastroenterology* **114**: 1133-1142

Yang W, Hendrickson WA, Crouch RJ and Satow Y (1990) Structure of

ribonuclease H phased at 2 A resolution by MAD analysis of the selenomethionyl

protein. *Science* **249**: 1398-1405

Zhu L, Salazar M and Reid BR (1995) DNA duplexes flanked by hybrid duplexes:

the solution structure of chimeric junctions in [r(cgcg)d(TATACGCG)]2.

Biochemistry **34**: 2372-2380

Figure legends

Figure 1: **Relative human RNase H1 initial cleavage rates and cleavage sites for the modified heteroduplex substrates.** (A) Successive substitution of MOE modified nucleotides at the 3'-pole of the ASO. (B) Successive substitution of MOE modified nucleotides at the 5'-pole of the ASO. Lines indicate the position of the human RNase H1 cleavages on the heteroduplex substrate. The length and thickness of the lines represent the intensity of the bands on the denaturing polyacrylamide gel for each respective cleavage site. Longer and thicker lines correspond to bands exhibiting greater intensity. Underlined sequences indicate the position of the MOE modified nucleotides. Heteroduplexes are shown with the sense oligoribonucleotide (above) oriented 5'→3' and chimeric ASO (below) 3'→5'. Ratio V_0 represents the initial cleavage rates for the modified heteroduplexes divided by the unmodified substrate. The V_0 values are an average of three measurements with estimated errors of CV < 10%. Initial cleavage rates were determined as described in the Materials and Methods.

Figure 2: **Cleavage pattern for heteroduplex A of various lengths.** Lines

indicate the position of the human RNase H1 cleavages on the heteroduplex

substrate. The length of the lines represents the intensity of the bands on the

denaturing polyacrylamide gel for each respective cleavage site. Longer lines

correspond to bands exhibiting greater intensity. Heteroduplexes are shown with

the sense oligoribonucleotide (above) oriented 5'→3' and the

oligodeoxyribonucleotide (below) 3'→5'.

Figure 3: **Initial cleavage rates and cleavage sites for chimeric ASO**

configurations of various heteroduplex sequences. (A) Initial cleavage rates

(V_0) and cleavage sites for heteroduplexes containing unmodified, 5-10-5 and 2-

10-8 chimeric ASOs. (B) Initial cleavage rates and cleavage sites for

heteroduplexes containing chimeric and unmodified ASO with similar 3'-DNA

termini. Lines and underlined sequences are as described in figure 1.

Heteroduplexes are shown with the sense oligoribonucleotide (above) oriented

5'→3' and chimeric ASO (below) 3'→5'. The initial cleavage rates were

determined as described in figure 1.

Figure 4: **Potency of heteroduplex C 5-10-5 and 2-10-8 ASOs in cultured**

cells. bEND cells were transfected with the 5-10-5 and 2-10-8 anti-TRADD ASOs

of heteruplex C as described in the Material and Methods. The TRADD mRNA

levels were determined for various ASO concentrations by quantitative RT-PCR.

Results were plotted with percent normalized mRNA versus ASO concentrations

for the 5-10-5 ASO (squares) and the 2-10-8 ASO (trangles). The bars represent

S.D. of the mean of three treatment groups. IC_{50} (shown bellow the graph) were

calculated from non-linear least-squares fit of the data.

Figure 5: **Initial cleavage rates and cleavage sites for Okazaki-like**

substrates. Heteroduplexes are shown with the chimeric sense oligonucleotide

(above) oriented 5'→3' and oligodeoxyribonucleotide (below) 3'→5'. The

underlined sequences indicate the positions of the ribonucleotide residues. The

substrates consisted of heteroduplexes containing ten (A-10/10) and fifteen (A-

15/5) ribonucleotides at the 5'-pole of the sense oligonucleotide with contiguous

stretches of, respectively, ten and five deoxyribonucleotides at the 3'-pole the

sense oligonucleotide. Lines are as described in figure 1. Ratio V_0 were

determined as described in figure 1.

Figure 6: **Model for the interaction of RNase H1 with the heteroduplex**

substrate containing MOE modifications at the 3' and 5'-poles of the ASO.

The green and blue lines represent, respectively, the sense oligoribonucleotide

oriented 5'→3' and chimeric ASO 3'→5'. The green and red boxes represent,

respectively, MOE residues at the 3' and 5'-poles of the ASO. The binding

interaction for human RNase H1 is shown with the RNA-binding domain (RNA-

BD) of the enzyme positioned 5' to the catalytic domain (Cat) on the

oligoribonuleotide. Each observed cleavage site on the RNA is coupled to a

specific binding interaction between the RNA-binding domain (RNA-BD) and the

3'-DNA/5'-RNA pole of the heteroduplex substrate. (A) Alteration in helical

geometry or steric interference by the MOE substitutions at the 3'-pole of the

ASO disrupts the binding interaction between the RNA-binding domain and the

heteroduplex resulting in the observed ablation of catalytic activity at the 5'-most

cleavage sites on the RNA. (B) MOE substitutions at the 5'-pole of the ASO are

positioned adjacent to the catalytic domain of enzyme.

Heteroduplex A	Cleavage Sites	Ratio V_0 (modified/unmodified)
Unmodified	5'-ACUGUGCGUGGAAAGCGUAG 3'-TGACACGCACCTTTCGCATC	1.00
19-1	5'-ACUGUGCGUGGAAAGCGUAG 3'-TGACACGCACCTTTCGCATC	0.69
18-2	5'-ACUGUGCGUGGAAAGCGUAG 3'-TGACACGCACCTTTCGCATC	0.46
17-3	5'-ACUGUGCGUGGAAAGCGUAG 3'-TGACACGCACCTTTCGCATC	0.47
16-4	5'-ACUGUGCGUGGAAAGCGUAG 3'-TGACACGCACCTTTCGCATC	0.37
15-5	5'-ACUGUGCGUGGAAAGCGUAG 3'-TGACACGCACCTTTCGCATC	0.40
14-6	5'-ACUGUGCGUGGAAAGCGUAG 3'-TGACACGCACCTTTCGCATC	0.34
13-7	5'-ACUGUGCGUGGAAAGCGUAG 3'-TGACACGCACCTTTCGCATC	0.41
12-8	5'-ACUGUGCGUGGAAAGCGUAG 3'-TGACACGCACCTTTCGCATC	0.47
11-9	5'-ACUGUGCGUGGAAAGCGUAG 3'-TGACACGCACCTTTCGCATC	0.59
10-10	5'-ACUGUGCGUGGAAAGCGUAG 3'-TGACACGCACCTTTCGCATC	0.53
9-11	5'-ACUGUGCGUGGAAAGCGUAG 3'-TGACACGCACCTTTCGCATC	0.38
8-12	5'-ACUGUGCGUGGAAAGCGUAG 3'-TGACACGCACCTTTCGCATC	0.01
7-13	5'-ACUGUGCGUGGAAAGCGUAG 3'-TGACACGCACCTTTCGCATC	0
6-14	5'-ACUGUGCGUGGAAAGCGUAG 3'-TGACACGCACCTTTCGCATC	0

Figure_1A

Figure_1B

Heteroduplex A	Cleavage Sites	Ratio V_0 (modified/unmodified)
Unmodified	5'-ACUGUGCGUGGAAAGCGUAG 3'-TGACACGCACCTTTCGCATC	1.00
1-19	5'-ACUGUGCGUGGAAAGCGUAG 3'-TGACACGCACCTTTCGCAT<u>C</u>	0.85
2-18	5'-ACUGUGCGUGGAAAGCGUAG 3'-TGACACGCACCTTTCGCA<u>TC</u>	0.59
3-17	5'-ACUGUGCGUGGAAAGCGUAG 3'-TGACACGCACCTTTCGC<u>ATC</u>	0.52
4-16	5'-ACUGUGCGUGGAAAGCGUAG 3'-TGACACGCACCTTTCG<u>CATC</u>	0.46
5-15	5'-ACUGUGCGUGGAAAGCGUAG 3'-TGACACGCACCTTTC<u>GCATC</u>	0.36
6-14	5'-ACUGUGCGUGGAAAGCGUAG 3'-TGACACGCACCTTT<u>CGCATC</u>	0.46
7-13	5'-ACUGUGCGUGGAAAGCGUAG 3'-TGACACGCACCTT<u>TCGCATC</u>	0.40
8-12	5'-ACUGUGCGUGGAAAGCGUAG 3'-TGACACGCACC<u>TTTCGCATC</u>	0.32
9-11	5'-ACUGUGCGUGGAAAGCGUAG 3'-TGACACGCACC<u>TTTCGCATC</u>	0.28
10-10	5'-ACUGUGCGUGGAAAGCGUAG 3'-TGACACGCACC<u>TTTCGCATC</u>	0.30

A-10   5'-ACUGUGCGUG
       3'-TGACACGCAC

A-15   5'-ACUGUGCGUGGAAAG
       3'-TGACACGCACCTTTC

A-20   5'-ACUGUGCGUGGAAAGCGUAG
       3'-TGACACGCACCTTTCGCATC

A-30   5'-ACUGUGCGUGGAAAGCGUAGACAAGGAGAU
       3'-TGACACGCACCTTTCGCATCTGTTCCTCTA

A-40   5'-ACUGUGCGUGGAAAGCGUAGACAAGGAGAUGCAGGUAUUG
       3'-TGACACGCACCTTTCGCATCTGTTCCTCTACGTCCATAAC

Figure_2

Heteroduplex		Cleavage Sites	$V_0(nM\ min^{-1})$
A	Unmodified	ACUGUGCGUGGAAAGCGUAG TGACACGCACCTTTCGCATC	6.02 ± 0.08
	5-10-5	ACUGUGCGUGGAAAGCGUAG TGACACGCACCTTTCGCATC	0.78 ± 0.28
	2-10-8	ACUGUGCGUGGAAAGCGUAG TGACACGCACCTTTCGCATC	3.31 ± 0.09
B	Unmodified	UAAUUCACAGAAUAGCACAA ATTAAGTGTCTTATCGTGTT	4.44 ± 0.09
	5-10-5	UAAUUCACAGAAUAGCACAA ATTAAGTGTCTTATCGTGTT	3.98 ± 0.05
	2-10-8	UAAUUCACAGAAUAGCACAA ATTAAGTGTCTTATCGTGTT	2.76 ± 0.06
C	Unmodified	CUGGCCUACGAGUAUGAGCG GACCGGATGCTCATACTCGC	2.96 ± 0.08
	5-10-5	CUGGCCUACGAGUAUGAGCG GACCGGATGCTCATACTCGC	2.71 ± 0.02
	2-10-8	CUGGCCUACGAGUAUGAGCG GACCGGATGCTCATACTCGC	1.13 ± 0.02
D	Unmodified	GAAGUAAGGACCAGAGACAA CTTCATTCCTGGTCTCTGTT	2.68 ± 0.09
	5-10-5	GAAGUAAGGACCAGAGACAA CTTCATTCCTGGTCTCTGTT	1.11 ± 0.06
	2-10-8	GAAGUAAGGACCAGAGACAA CTTCATTCCTGGTCTCTGTT	0.78 ± 0.03
E	Unmodified	UCAAAUCCAGAGGCUAGCAG AGTTTAGGTCTCCGATCGTC	2.77 ± 0.06
	5-10-5	UCAAAUCCAGAGGCUAGCAG AGTTTAGGTCTCCGATCGTC	2.12 ± 0.06
	2-10-8	UCAAAUCCAGAGGCUAGCAG AGTTTAGGTCTCCGATCGTC	1.11 ± 0.06
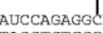
Figure_3A

Heteroduplex	Cleavage Sites	V_0 (nM min^{-1})

A
- 5-10-5
  ACUGUGCGUGGAAAGCGUAG
  TGACACGCACCTTTCGCATC — 0.78 ± 0.28
- 10-deoxy
  ACUGUGCGUGGAAAGCGUAG
  CGCACCTTTC — 6.41 ± 0.09

B
- 5-10-5
  UAAUUCACAGAAUAGCACAA
  ATTAAGTGTCTTATCGTGTT — 3.98 ± 0.05
- 10-deoxy
  UAAUUCACAGAAUAGCACAA
  GTGTCTTATC — 11.86 ± 0.30
- 20-deoxy
  UAAUUCACAGAAUAGCACAAACUAC
  GTGTCTTATCGTGTTTGATG — 11.15 ± 0.22

C
- 5-10-5
  CUGGCCUACGAGUAUGAGCG
  GACCGGATGCTCATACTCGC — 2.71 ± 0.02
- 20-deoxy
  CUGGCCUACGAGUAUGAGCGUGAUG
  GATGCTCATACTCGCACTAC — 4.86 ± 0.09

D
- 5-10-5
  GAAGUAAGGACCAGAGACAA
  CTTCATTCCTGGTCTCTGTT — 1.11 ± 0.06
- 10-deoxy
  GAAGUAAGGACCAGAGACAA
  TTCCTGGTCT — 7.65 ± 0.11
- 20-deoxy
  GAAGUAAGGACCAGAGACAAAAAAGG
  TTCCTGGTCTCTGTTTTTCC — 6.17 ± 0.06
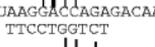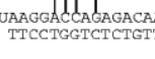
E
- 5-10-5
  UCAAAUCCAGAGGCUAGCAG
  AGTTTAGGTCTCCGATCGTC — 2.12 ± 0.06
- 10-deoxy
  UCAAAUCCAGAGGCUAGCAG
  AGGTCTCCGA — 7.14 ± 0.08
- 20-deoxy
  UCAAAUCCAGAGGCUAGCAGUUCAU
  AGGTCTCCGATCGTCAAGTA — 6.64 ± 0.17
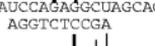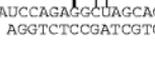
Figure_3B
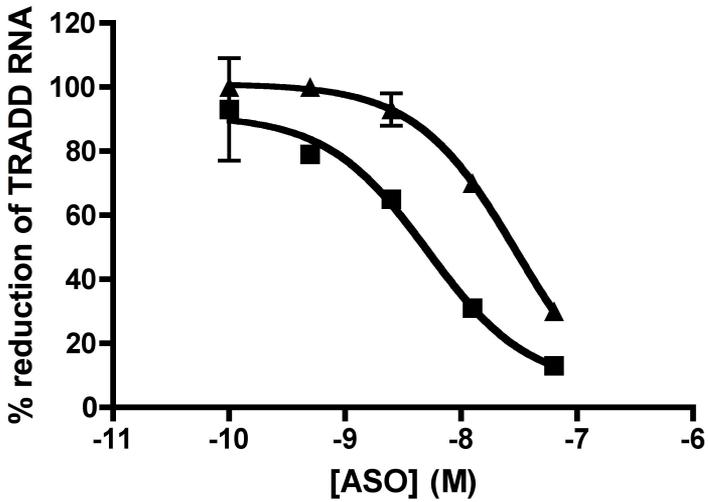
Fig. 4

Heteroduplex A	Cleavage Sites	Ratio V_0 (nM min^{-1})

A-20

5'-ACUGUGCGUGGAAAGCGUAG
3'-TGACACGCACCTTTCGCATC

1.00

A-15/5

5'-ACUGUGCGUGGAAAGCGUAG
3'-TGACACGCACCTTTCGCATC

0.87

A-10/10

5'-ACUGUGCGUGGAAAGCGUAG
3'-TGACACGCACCTTTCGCATC

1.02

Figure_5

A

3'-MOE

B

5'-MOE

Figure_6AB